 doi:10.20944/preprints202106.0140.v2

The connection between RF anisotropy of acoustically excited NaCl aqueous solution and Debye ionic vibrational potential

Alexander V. Kramarenko[a], Andrey V. Kramarenko[b], Oksana O. Savenko[c,*]

[a]*TREDEX Company Ltd., PO box 11515, Kharkiv, Ukraine 61001*
[b]*General and Inorganic Chemistry Department, National Technical University "KhPI", 2 Kyrpychova str., Kharkiv, Ukraine 61002*
[c]*School of Physics and Technology, V. N. Karazin Kharkiv National University, 4 Svobody Sq., Kharkiv, Ukraine 61022*

Abstract

In this paper, we considered two phenomena in acoustically excited aqueous solutions of a strong electrolyte. These are the well-known Debye ionic vibrational potential (IVP), and radiofrequency anisotropy we discovered earlier , apparently, for the first time. Since both occur due to the accelerated motion of the solution, we have tried to combine them in one simple model. We have established that for a polarized UHF radio wave passed through a NaCl aqueous solution excited by an acoustic pulse the rotation angle of its vector $\overline{E}$ is proportional to the integral of the square of the observing IVP over time. An equivalent electrical circuit simulating the observed phenomena has been proposed and tested for physical feasibility. Several arguments are given in favour of the fluid-gyroscopic mechanism of RF anisotropy-related effects.

We also found out that the IVP is practically independent of the vibrational velocity for frequencies below 10 kHz and it tends to zero at zero frequency. The latter is consistent with the law of conservation of energy but contradicts the incomplete existing theory .

Keywords: aqueous electrolyte solution, UHF wave, polarization direction, Debye ionic vibrational potential, giant relaxation time

*Principal corresponding author
Email addresses: tredexcompany37@gmail.com (Alexander V. Kramarenko), andrii.kramarenko@khpi.edu.ua (Andrey V. Kramarenko), xana.savenko@gmail.com (Oksana O. Savenko)

Preprints (www.preprints.org) | NOT PEER-REVIEWED | Posted: 9 December 2021 doi:10.20944/preprints202106.0140.v2

1. Introduction

Earlier [1] we have published a brief description of a new radio-frequency method of remote studying of conductive liquid media. The method is based on the phenomenon, fixed by us, apparently, for the first time. We found that the UHF radio wave polarization direction rotates when it is passing through an electrolyte solution moving with acceleration. We first discovered this *in vivo* for radio waves passing through an experimenter's heart region. We recorded a contactless electrocardiogram [2, 3]. We then reproduced the phenomenon *in vitro* with normal saline, which was mechanically or acoustically excited.

Let us list all the phenomena we observed in the experiment [1]:

1. A 433 MHz radio wave polarization direction rotation after passing through the normal saline moving with acceleration. In other words, radiofrequency anisotropy was observed for it (but not for just distilled water);
2. The direction of polarization of the radio wave that passed through the saline, after a single acoustic impulse abruptly changed, then relaxed back to starting condition for a long time (about tens of seconds);
3. An alternating electric potential was generated between two AgCl electrodes immersed in a saline solution when it was excited by a sound wave.

There are still no mentions in literature exactly about the first phenomenon we discover earlier [1]. Maybe the closest effect for seawater is the "wake of a submarine" detected by radars [4]. The RF anisotropy also has been observed for solid ice [5–9] or liquid crystals [10] but never for rather unstructured aqueous solution.

The second phenomenon we observed is a kind of "memory" effect [11] described earlier for viscoelastic fluids [12], for example. For electrolyte solutions containing no particles revealing specific interactions (liquid crystals, polymers, colloids, etc.) this has also not been previously described to our knowledge.

The third phenomenon is well-known. An alternating electric potential between two points of an acoustically excited solution is the so-called Debye ionic vibrational potential (IVP). The IVP

Preprints (www.preprints.org) | NOT PEER-REVIEWED | Posted: 9 December 2021 doi:10.20944/preprints202106.0140.v2

phenomenon was theoretically predicted by Debye in 1933 [13]. It is generally accepted [14] that the Debye IVP in electrolyte solutions arises due to the difference in the inert masses of solvated cations and anions, as well as because of their different mobility in a viscous solvent. Debye also proposed [13] an equation expressing the dependence of the electric potential on the vibrational velocity. The equation did not take into account the electrophoretic and relaxation effects, as well as the frequency dependence of the permittivity and electrical conductivity of the solution at high frequencies. Eger, Bugosh, and Govorka [15] derived an equation that takes these effects into account, and in this form, they used it to process the first experimental data on IVP at an ultrasonic frequency of 265 kHz [16]. The Debye IVP has been measured for a lot of systems [14, 17, 18] but at ultrasonic frequencies only.

The potential we registered in [1] is of the same order of magnitude (up to tens of μV) as the Debye IVP. We have recorded it in the sound frequency range, which is not been done [14] before, except for a study by one of us (with co-authors) [19] reporting the occurrence of the IVP *in vivo* when recording a classical ECG. An IVP also occurred *in vitro* [19] with the movement of a free jet inside a vessel with saline. Considering the acceleration of liquid by heart or a piston pump as a very low-frequency sound wave we suppose it was the very first low-frequency IVP registration.

It should be noted that the problem of the frequency dependence of the Debye potential in a wide frequency range has never been a subject of a special study. The authors of [17] pointed out the virtual independence (NB!) of the IVP amplitude from the ultrasound frequency in the common measurement range (100 kHz-1 MHz), and this is well explained by the fact that the amplitude of the vibrational velocity does not depend on the frequency [20]. To check this prediction, we have attempted [1] to detect IVP appearance at as low a sound frequency as possible. Of course, it is limited by the noise of the measuring circuit we currently have. In [1] we have provided only plot of our final results. Here we are going to report both the measurement procedure in details.

2. Methods

2.1. RF wave polarimetry

The multistatic radar emitting a continuous monochromatic wave passing through the pericardial region has been implemented. The angle of polarization direction measurement procedure has

Preprints (www.preprints.org) | NOT PEER-REVIEWED | Posted: 9 December 2021 doi:10.20944/preprints202106.0140.v2

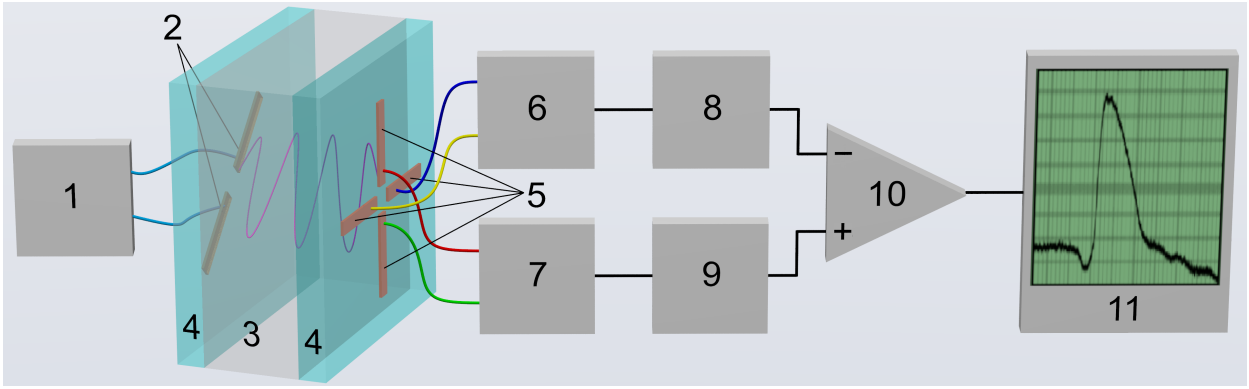

Figure 1: A simplified block diagram of the device for recording of RF wave polarization direction deviation [1]. 1 – a continuous wave transmitter 433.82 MHz, –12 dBm; 2 – transmitting antenna; 3 – an object studied; 4 – a dielectric material; 5 – orthogonal orientation quadrature antennas; 6 – channel X RF amplifier; 7 – channel Y RF amplifier; 8 – X channel amplitude logarithmic detector; 9 – Y channel amplitude logarithmic detector; 10 – instrumentation differential amplifier; 11 – registrating device (X axis is time, Y axis is deviation). The antennas are shown as Hertz's half-wave dipoles, it is clear that their real configuration will be different. Transmitting antenna is deviated at angle of 45°relative to both receiving ones.

been described in details earlier [1] so here we only provide a signal pathway block diagram (see Fig. 1). The calibration dependence has turned out to be linear enough within output signal range of $\pm 0.2\ V$:

$$\alpha \approx 45 + 37.8 U_{\text{out}} - 11.0 U_{\text{out}}^3. \tag{1}$$

where α is the polarization direction rotation angle, degrees; U_{out} is the operational amplifier output signal and 45° is the initial shift of transmitting antenna relatively to receiving crossed dipoles. This setup allows us to measure α in the first quadrant only due to the neglecting of any phase shift information between channels. However, we have never recorded the α value outside of the $45 \pm 30°$ range

2.2. Debye IVP measurement

In our previous work [1], a successful attempt to register the low-frequency Debye potential was made. Here we provide a simplified diagram of our installation (see figure 2).

Since Debye IVP and radio-frequency anisotropy occur in the solution under the same exci-

Preprints (www.preprints.org) | NOT PEER-REVIEWED | Posted: 9 December 2021 doi:10.20944/preprints202106.0140.v2

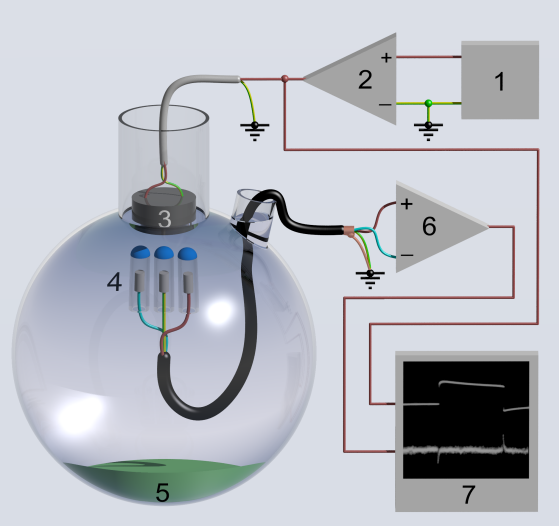

Figure 2: Installation for acoustoelectric effect registration. 1 - generator; 2 - power amplifier; 3 - emitter; 4 - silver chloride electrodes under protective caps; 5 - sound-absorbing cover; 6 - instrumental operational amplifier; 7 - recorder.

tation conditions, it would be correct, in our opinion, to consider a possible relationship between these phenomena.

3. Results and discussion

3.1. Debye IVP theory test

Let's first address the appearance of the Debye potential upon low-frequency acoustic excitation of the solution, assuming the effects of electric potential generation and the rotation of the Jones vector to be somehow interrelated, and perhaps this hypothesis will help us understand the cause of the radio frequency anisotropy.

To compare our results with existing theory we performed a calculation according to the formula 2 from [14]:

$$\frac{\Phi_0}{a_0} = \frac{c}{10N_A e}\left[\frac{t_+}{z_+}\left(W_+ - \frac{RT}{c^2}\right) - \frac{t_-}{z_-}\left(W_- - \frac{RT}{c^2}\right)\right] \cdot \frac{4\pi L_0}{\omega\varepsilon\sqrt{\left(\frac{\varepsilon_\omega}{\varepsilon}\right)^2 + \left(\frac{4\pi L_\omega}{\omega\varepsilon}\right)^2}} \tag{2}$$

where Φ_0 is an amplitude of an arising potential, μV; a_0 is the solvent vibrational velocity amplitude , cm/s; c is the sound wave propagation speed in solution, cm/s; N_A is Avogadro's number,

Preprints (www.preprints.org) | NOT PEER-REVIEWED | Posted: 9 December 2021 doi:10.20944/preprints202106.0140.v2

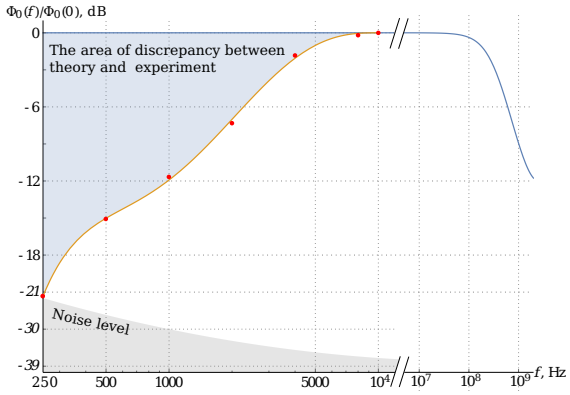

Figure 3: FRF of the recorded signal. Red dots - experimental results, blue curve - calculated data for 0.9% NaCl solution at 22°C in accordance with the basic theory [14, 15]

mol^{-1}; e is the charge of the electron, C; t_+, t_-, z_+, z_- are the transference numbers and charge moduli of cation and anion, respectively; W_+ and W_- are apparent molar masses of the cation and anion, g/mol; ω is the circular vibration frequency, rad/s; L_0 and L_ω are the electrical conductivities of the solution at zero frequency and at circular frequency ω, respectively, CGS-ESU; ε and ε_ω are the solvent permittivities at the same frequencies for a 0.9% NaCl solution at a temperature of 22°C.

The temperature and frequency dependences of the dielectric constant of the solvent, and the electrical conductivity of the solution, as well as the speeds of sound in it, required for the calculation, were taken from [21–23].

Results of the calculation versus the data of our measurements are shown in the Fig.3. The predictions of the theory totally contradict our experiment in the low-frequency region, the recorded FRF of the Debye effect is very different in the low-frequency region from the theoretically estimated.

At frequencies above 100 MHz, theory [15] predicts a decrease in the amplitude of the IVP due to the inertness of massive ions. In the high-frequency region, the Debye potential can also be shunted by the parasitic capacitance of the solution, especially at low electrolyte concentrations [14]. In the low-frequency region, the theory predicts a constant non-zero IVP amplitude at a frequency tending to zero (NB!), what is absolutely impossible due to energy restraints as

Preprints (www.preprints.org) | NOT PEER-REVIEWED | Posted: 9 December 2021 doi:10.20944/preprints202106.0140.v2

maintaining a constant potential in an electrically conductive medium requires continuous energy consumption. In other words, the ohmic resistance of the solution shunts the emerging potential at low frequencies (similar to the capacitance in the high-frequency region), what the existing theory [14, 15] does not take into account. Apparently, the basic theory [14, 15, 17] did not pay much attention to low-frequency processes, the more so as the registration [16, 17] of low-level signals in the absence of specialized instrumental low-noise operational amplifiers at such frequencies was an issue at that time.

While the Debye potential has rapid "roll-off" at low frequencies, this effect is not observed for the RF polarization vector, i.e. unlike the electric potential, RF anisotropy behaves quite differently.

3.2. Connection of RF anisotropy and Debye IVP

To compare the Debye IVP and RF anisotropy in the time domain, we used the Heaviside function as an analytical signal (see Fig.4).

In the case of excitation in the form of a Heaviside function, the exponential decay in the Debye potential is due to ohmic shunting at low frequencies, while the explanation of the Jones vector behavior is not so obvious. Indeed, any deviation of an isotropic medium from thermodynamic equilibrium relaxes with time exponentially [24], and one could consequently expect the Jones vector, like the Debye potential, would be asymptotically approaching the initial position over time. However, instead of this, "memorizing" of the position of the maximum deviation happens for some time (on the order of units/tens of seconds), followed by normal relaxation. Therefore,

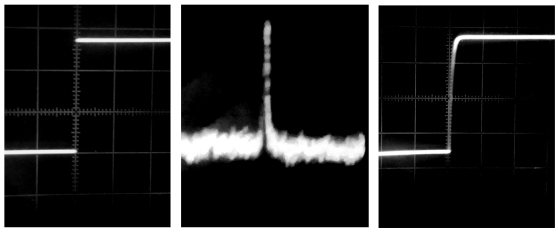

Figure 4: On the left - the Heaviside signal fed to the hydroacoustic emitter, in the center - the Debye potential U = 20 μV, on the right - the rotation of the Jones vector (all images are captured from the oscilloscope screen)

Preprints (www.preprints.org) | NOT PEER-REVIEWED | Posted: 9 December 2021 doi:10.20944/preprints202106.0140.v2

in the very mechanism of the solution anisotropy change, there must be an integration process, or rather, something similar to an analog sample and hold circuit.

Let's take that no chemical or physical processes in the solution add "external" energy [1], and its only source is an acoustic wave. At the same time, as an initial condition, it is necessary to exclude the hypothesis of rotation of the polarization vector under the influence of any electric potential applied to the solution, the Debye potential in particular. For this, we carried out experiments with passing an electric current through the solution in the frequency band from 0 Hz to 10 kHz, and voltages from 0 to 2 V. No of them caused any deviations of the RF polarization vector, though the signal level in the experiment exceeded the Debye potential recorded on the same setup (Fig. 3) by 116 dB. This allows us to make an unambiguous conclusion: the polarization vector of the radio-frequency signal passing through the solution does not rotate under the influence of an applied voltage. Thus, we can accept that the "electric part" of the Debye effect cannot be the root of the radio frequency anisotropy; it would be more correct to assume that the mechanism that "triggers" the Debye effect can also trigger the rotation of the RF signal polarization.

The system relaxation after the acoustic wavefront passage can be modeled by an ideal differentiating circuit. The Debye process (given its experimental frequency response recorded by us in the low-frequency region) can also be described in the time domain by a differentiating circuit.

We also assume that some "X" process, which is responsible for the rotation of the polarization direction, has the power flux density proportional to the square of Debye IVP (considering no significant reactive component in the load). Then the "X" process model can be represented in the form of the following electrical circuit (Fig. 5).

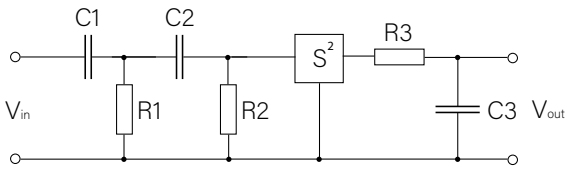

Figure 5: The simplified electrical circuit of the proposed model of the process. The C_1R_1 circuit simulates the energy dissipation of an acoustic wave, the C_2R_2 circuit - lower band limitation for the Debye effect, S^2 - a square-law generator, the C_3R_3 circuit - a hypothetical integrator, which physical nature is under investigation

Preprints (www.preprints.org) | NOT PEER-REVIEWED | Posted: 9 December 2021 doi:10.20944/preprints202106.0140.v2

Of course, the transfer function of ideal differentiating circuits does not satisfy the conditions of physical feasibility [25]. However, in our case, the energy of the acoustic wave is finite by definition what makes it possible to use ideal circuit as a model in which the corresponding differentiation time constants are $\tau_1 = R_1C_1$, $\tau_2 = R_2C_2$ while the integration time constant $\tau_3 = R_3C_3$. Assuming $\theta = \frac{\tau_1\tau_2}{2(\tau_1+\tau_2)}$ the analytical solution can be derived for the rotation angle of the polarization direction $\Delta\alpha$ as follows:

$$\Delta\alpha \simeq \int_{t-\tau_3}^{t} \left(e^{-\frac{t}{\tau_1}} \cdot e^{-\frac{t}{\tau_2}}\right)^2 dt = \int_{t-\tau_3}^{t} \exp\left(-\frac{t}{\theta}\right) dt = \theta\left[\exp\left(\frac{\tau_3 - t}{\theta}\right) - \exp\left(-\frac{t}{\theta}\right)\right] \quad (3)$$

Let's also check if the model is physically feasible and stable. To do this we will use the Laplace transform. The complex transfer function of the series-connected cascades is equal to the product of the complex transfer functions of all the in-series cascades; in our case, this means

$$H(s) = H_1(s) \cdot H_2(s) \cdot H_3(s) \quad (4)$$

The transfer function of the circuit 5 can be written as follows:

$$H = s^2\tau_1\tau_2 \cdot \left[1 + s(\tau_1 + \tau_2 + \tau_3) + s^2(\tau_1\tau_2 + \tau_1\tau_3 + \tau_2\tau_3) + s^3 \cdot \tau_1\tau_2\tau_3\right]^{-1} \quad (5)$$

See appendix Appendix A for the detailed calculations.

Since the given circuit is a modeling one, the values of resistances and capacitances cannot be absolutely random, namely it is necessary to adhere to the following relations over the numerical calculation of the transfer function: $C_1 \gg C_2 \gg C_3; R_3 \gg R_2 \gg R_1$. Let's take the following values for example: $R_1 = 1$ Ohm, $R_2 = 100$ Ohm, $R_3 = 10$ kOhm, $C_3 = 50\mu$F, $C_2 = 0.5$ mF, $C_1 = 50$ mF. The poles of the transfer function (on the complex s-plane) are located at point (-2) on the real axis and have a zero imaginary coordinate, while its zero is at the origin point (see Fig. 6).

Now we can argue that the model is physically feasible, stable [26], and ready to work. Let's check the results of a software simulation on the system response to the Heaviside signal. The Debye IVP original signal and the rotation of the RF wave polarization direction in the time domain are shown on Fig. 7.

As one can see, software simulation provides a satisfactory fit between the real and waveforms synthesized by the model. The negligible difference is due to the not quite accurate selection of the time parameters, which was carried out, of course, empirically.

Preprints (www.preprints.org) | NOT PEER-REVIEWED | Posted: 9 December 2021 doi:10.20944/preprints202106.0140.v2

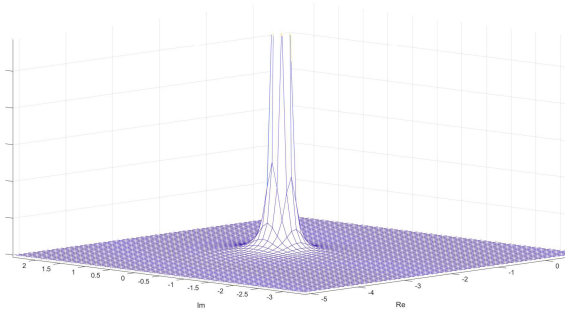

Figure 6: Complex s-plane mapping of the signal

It is clear that analogy is not proof, so for now, only a provident conclusion can be drawn: some physical process “X”, which has properties of an integrating circuit, can transform the energy of an acoustic signal in such a way that the radio-frequency polarization vector changes its position and remembers it to some, quite significant, time.

The physical structure of this integrator cannot be electrical or molecular for the reasons stated earlier (in [1] as well). Then, according to the principle of exclusion, it would be acceptable to assume the gyroscopic mechanism of the observed effect.

3.3. The gyroscopic hypothesis

However, it should be taken into account that we cannot use some basic concepts: for instance, instead of considering an object as isotropic, it will be essential to introduce either the concept of

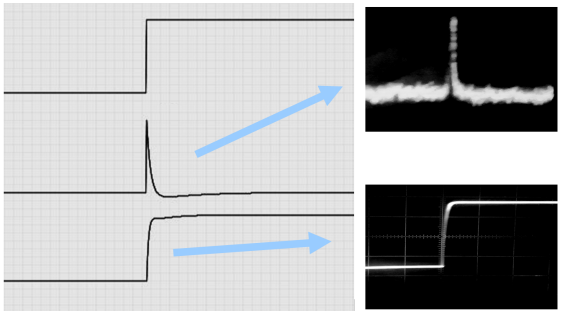

Figure 7: The upper curve is the Heaviside signal, in the middle - Debye potential, in the bottom - rotation of the RF signal polarization vector. Real experimental curves are shown on the right for comparison.

 doi:10.20944/preprints202106.0140.v2

orthotropy of a solution in the receiving plane (i.e. there is always anisotropy in a resting solution, and upon excitation of the solution it can change) or explain its occurrence in our experiments in some other way.

Meanwhile, it will be also needed to assume the system's invariance in time. Moreover, when considering the memory effect, one will also have to discard the hypothesis of ergodicity [27].

Let's ground the foregoing. It is known that the electrical conductivity of classical electrolyte solutions is, by definition, isotropic property that does not depend on the history of the system (within the framework of the immanent hypothesis, the deviation of the polarization angle is functionally associated with electrical conductivity). However, in the result of our experiments, two phenomena contradicting this statement were found, namely:

Rotation of the plane of polarization, i.e. the presence of a path difference between the ordinary and extraordinary waves inside the solution. If the electrical conductivity remained isotropic, any of its simultaneous (or infinitely slow) change for the entire solution would rotate the plane of polarization in no way. It seems that in our case, the electrical conductivity transforms into a tensor changing over time. Such a phenomenon, so far, has been observed either for crystals with preferential directions or for specifically oriented structures [28, 29]

Presence of a long-term "memory" of the system. Classical physical chemistry of electrolyte solutions studies the solution in thermodynamic equilibrium. Moreover, all the integral properties of such a solution are state functions, i.e., by definition, they do not depend on the system history. To transport properties (not thermodynamic but rather kinetic, such as electrical conductivity) over long time intervals are also considered as state functions. This is an implication of the ergodicity [27] of the system, i.e. the equivalence of the average over the volume of the entire system at a certain instant of time and the average of a small part of this system over a sufficiently long time period. Simply put, if one looks at a very small piece of a system long enough, one can get an accurate depiction of the properties of the entire system. Ergodic systems, by definition, have no memory, and the average values of the properties of such systems do not depend on their prehistory.

In our experiments, nothing of that kind is observed. The system demonstrates the dependence of the properties on prehistory at macroscopic time intervals (at least tens of seconds). Such prop-

Preprints (www.preprints.org) | NOT PEER-REVIEWED | Posted: 9 December 2021 doi:10.20944/preprints202106.0140.v2

erties are more typical for polymers [30], and the description of such systems has been arousing steady interest for a long time [11, 31].

Obviously, the classical thermodynamic equilibrium (or close to it) description of a solution is not applicable here at all. A correct description of such a system requires the use of non-equilibrium thermodynamics. In addition, such systems radically cannot be simulated by the classical Monte Carlo method since the coordinates and momenta of particles in a non-ergodic system are correlated, and the behavior of the particles in time is not a Markov chain. Therefore, in our work, we will rely solely on experimental data and apply the required mathematical apparatus "on demand."

Indeed, if the pendulum gyrocompass is placed in a gravitational field for a moment, then it'll start to change the orientation of the angular momentum vector. If in a moment we "turn off gravitation", then the gyrocompass will perform the functions of a gyroscope, i.e. hold the position of the rotation axis [32]. According to the principle of equivalence, if we replace gravity with the corresponding acceleration, then the gyrocompass will behave in the same way.

Liquid gyroscopes utilizing acidified water or aqueous solutions of lithium salts as a working medium are well known [33], it is also known that any vibrations (NB!) are an undesirable effect for them, but the reports on experiments propagating an acoustic wave through the working medium were not found by us.

However, a precondition of such gyroscopes operation is a radio-frequency field, which presence leads to the precession of the working body nuclei. In our case, however, the effect doesn't depend on the field strength, i.e. we have to assume that the rotation of the RF signal polarization vector is due to a change in either the electronic moment of the atoms or the magnetic moment of the nuclei of ions with an odd mass number. How an acoustic wave can affect the rotation of the magnetic moment carriers is yet unclear for us; large-scale experimental and theoretical studies are absolutely necessary.

So, based on the simulation results, we assume that the discussed process "X" can consistently fit into the framework of known physical effects. An additional argument in favor of the "gyroscopic" hypothesis may be the "saturation effect" which was discovered in our experimental work as the radio-frequency polarization vector under the influence of the acoustic wave was shifted

Preprints (www.preprints.org) | NOT PEER-REVIEWED | Posted: 9 December 2021 doi:10.20944/preprints202106.0140.v2

at a certain angle increasing less and less whereas the wave amplitude rises, and the process of polarization vector deviation never turned into rotation.

It can also be assumed that the changing of the electronic and/or nuclear moment orientation under the influence of external acceleration always occurs in water, and electrolyte ions are needed only to register the deviation of the polarization vector in the radio frequency range. If this assumption is faithful, then it will be necessary to re-examine numerous existing ideas about the behavior of aquatic environments. For example, the physics of the "wake of a submarine" detected by radars [4], the biophysical mechanism of cardiac electrical signals generation [19], and many other phenomena.

4. Conclusion

Within the theoretical framework, we tried to provide some reasoning and explanation of the processes observed in our previous experiments [1], which occur under any mechanical excitation in solutions of strong electrolytes, namely low-frequency Debye ionic vibration potential, radio-frequency anisotropy and its conservation. The independence of the RF anisotropy appearance from the applied voltage and from the Debye potential in particular has been proved experimentally.

Simulation of the observed effects with the equivalent electrical circuit (see Fig. 5) allows us to make a provident conclusion that some physical process "X", which has properties of an integrating circuit, can transform the energy of an acoustic signal in such a way that the radio-frequency polarization vector changes its position and remembers it to some, quite significant, time (see Fig. 7).

Given the futility of describing the "memory" effect as a process of electrical or molecular origin, several arguments were presented in favor of the fluid-gyroscopic mechanism. It was suggested that the rotation of the polarization vector of the RF signal is due to the change in the electric moment of the liquid atoms and/or the nuclear moment of ions having an odd mass number.

The basic theory of the ionic vibrational potential was discussed, namely, its predictions in the low-frequency range, and their discrepancy with the energy conservation law and experiment was highlighted.

Preprints (www.preprints.org) | NOT PEER-REVIEWED | Posted: 9 December 2021 doi:10.20944/preprints202106.0140.v2

We assume that the occurrence of the low-frequency Debye ionic vibration potential and the deviation of the RF polarization vector are conjugated, but only in the sense that the power flux density of some physical process "X" responsible for the rotation of the polarization vector is proportional to the square of the electric potential voltage.

Implicitly that laboratory equipment and adequate working conditions are required to continue work in this direction and obtain accurate proving, what is not the authors' case. Nevertheless, some promising engineering devices (in addition to those described in our previous, experimental, paper) are likely. E.g. it was found that the anisotropy of the solution is transported by the carrier (Sic!), i.e. if one pumps the solution which changed the polarization vector under acoustic disturbance, then the trace of the disturbance is preserved. This phenomenon makes it possible to develop a completely contactless unitary sensor of velocity and liquid inhomogeneities (the experimental model has already shown the feasibility of such an idea even for tap water).

Appendix A. Transfer function calculation

Given the equation 4, let's look at the transfer functions of each of the three introduced four-poles below.

EMF source $\varepsilon(t)$ is connected to the input of the first four-pole. Since the resistance of the capacitor is reactive, let's move to the frequency domain and write the equation for the first circuit:

$$E(j\omega) = I(j\omega) \cdot \left(R_1 + \frac{1}{j\omega C_1} \right)$$

Here and in the following, it is convenient to introduce a complex variable with zero real part $s = j\omega$.

The complex transfer function is defined as the ratio of the system output to its input:$H(s) = \frac{X_out(s)}{X_in(s)}$. In the first circuit under consideration, the input is the voltage $E(s)$, and the output is the voltage U_1 across the resistor R_1. Let's find this voltage, it is equal to the product of the current $I(s)$ by the resistance R_1. The current $I(s)$, in turn, is defined as the ratio of the EMF $E(s)$ to the total resistance of the circuit, i.e.

$$I(s) = \frac{E(s)}{R_1 + \frac{1}{sC_1}}$$

Preprints (www.preprints.org) | NOT PEER-REVIEWED | Posted: 9 December 2021 doi:10.20944/preprints202106.0140.v2

Accordingly, the output voltage of the system

$$U_1 = I(s) \cdot R_1 = \frac{E(s)R_1}{R_1 + \frac{1}{sC_1}}$$

Coming back to the definition of the complex transfer function, we obtain

$$H_1 = \frac{E(s)}{U_1(s)} = \frac{R_1}{R_1 + \frac{1}{sC_1}}$$

Analysis of the two next four-poles shares the same insights, except for the fact that there's a transition from instantaneous voltage to power in the third cascade, i.e.

$$H_2 = \frac{U_1(s)}{U_2(s)} = \frac{R_2}{R_2 + \frac{1}{sC_2}}$$
$$H_3 = \frac{P_2(s)}{P_3(s)} = \frac{1/sC_3}{R_3 + 1/sC_3}$$

Owning definitions of all three transfer functions, let's write the expression for the entire system:

$$H = \frac{R_1}{R_1 + 1/sC_1} \cdot \frac{R_2}{R_2 + 1/sC_2} \cdot \frac{1/sC_3}{R_3 + 1/sC_3}$$

For the subsequent reduction of similar ones, it is convenient to introduce a new constant $\tau = RC$ - the time constant of the RC-circuit. Then, we obtain the formula 5 given in section 3.2:

$$H = \frac{\tau_1\tau_2 \cdot s^2}{(1+\tau_1 s)\cdot(1+\tau_2 s)\cdot(1+\tau_3 s)} =$$
$$\frac{\tau_1\tau_2 \cdot s^2}{(1+\tau_2 s+\tau_1 s+\tau_1\tau_2 s^2)\cdot(1+\tau_3 s)} =$$
$$\frac{\tau_1\tau_2 \cdot s^2}{1+\tau_2 s+\tau_1 s+\tau_1\tau_2 s^2+\tau_3 s+\tau_2\tau_3 s^2+\tau_1\tau_3 s^2+\tau_1\tau_2\tau_3 s^3} =$$
$$\frac{s^2 \cdot \tau_1\tau_2}{1+s(\tau_1+\tau_2+\tau_3)+s^2(\tau_1\tau_2+\tau_1\tau_3+\tau_2\tau_3)+s^3\cdot\tau_1\tau_2\tau_3}$$

References

[1] A. V. Kramarenko, A. V. Kramarenko, O. Savenko, A new radio-frequency acoustic method for remote study of liquids, Scientific Reports 11 (2021) 6696. doi:10.1038/s41598-021-84500-6.

[2] A. V. Kramarenko, accessed: Jul 23, 2020, Demo of non-contact polarimetric cardiograph testing, URL: https://youtu.be/gOGvGjJ2QnI.

[3] A. V. Kramarenko, accessed: Oct 13, 2020, Demo of a car driver monitoring system, URL: https://youtu.be/yB9uKd3MNxU.

[4] M. Zhang, J. Wang, Microwave scattering from submerged object induced wake over rough sea surface, in: 2017 XXXIInd General Assembly and Scientific Symposium of the International Union of Radio Science (URSI GASS), 2017, pp. 1–4. doi:10.23919/URSIGASS.2017.8105396.

[5] M. I. Finkel'shteyn, V. G. Gloushnev, A. N. Petrov, On the anisotropy of the radiowave attenuation in the sea ice, International Meeting on Radioglaciology, Lyngby, May 1970. Proceedings, 1970. URL: https://www.coldregions.org/vufind/Record/40737.

[6] E. I. Kaleri, A. M. Kluga, A. N. Petrov, M. I. Finkel'shteyn, Anisotropy of radiowave delay in sea ice (1971). URL: https://www.coldregions.org/vufind/Record/41749.

[7] V. V. Bogorodskiy, G. P. Khokhlov, Anisotropy of the microwave dielectric constant and absorption coefficient of arctic drift ice (1977). URL: https://www.coldregions.org/vufind/Record/87543.

[8] K. Matsuoka, T. Furukawa, S. Fujita, H. Maeno, S. Uratsuka, R. Naruse, O. Watanabe, Crystal orientation fabrics within the antarctic ice sheet revealed by a multipolarization plane and dual-frequency radar survey, Journal of Geophysical Research: Solid Earth 108 (2003). URL: https://agupubs.onlinelibrary.wiley.com/doi/abs/10.1029/2003JB002425. doi:10.1029/2003JB002425. arXiv:https://agupubs.onlinelibrary.wiley.com/doi/pdf/10.1029/2003JB002425.

[9] C. Wang, Z. Dong, X. Zhang, X. Liu, G. Fang, Method for anisotropic crystal-orientation fabrics detection using radio-wave depolarization in radar sounding of mars polar layered deposits, IEEE Transactions on Geoscience and Remote Sensing 56 (2018) 5198–5206. URL: https://ieeexplore.ieee.org/document/8355720.

[10] S. Missaoui, M. Kaddour, A novel combined-design of an antenna-filter rf with optical anisotropy of nematic liquid crystal for uwb applications, OPTOELECTRONICS AND ADVANCED MATERIALS-RAPID COMMUNICATIONS 13 (2019) 209–216. URL: https://oam-rc.inoe.ro/articles/a-novel-combined-design-of-an-antenna-filter-rf-with-optical-anisotropy-of-nematic-liquid-crysta fulltext.

[11] B. D. Coleman, Thermodynamics of materials with memory, Archive for Rational Mechanics and Analysis 17 (1964) 1–46. doi:10.1007/BF00283864.

[12] D. D. Joseph, Fluid Dynamics of Viscoelastic Liquids, Springer-Verlag Berlin Heidelberg GmbH, 1990.

[13] P. Debye, A method for the determination of the mass of electrolytic ions, The Journal of Chemical Physics 1 (1933) 13. doi:10.1063/1.1749213.

[14] R. Zana, E. B. Yeager, Ultrasonic Vibration Potentials, in: J. O. Bockris, B. E. Conway, R. E. White (Eds.), Modern Aspects of Electrochemistry, Springer, Boston, MA, 1982, pp. 1–60. doi:10.1007/978-1-4615-7458-3_1.

[15] J. Bugosh, E. Yeager, F. Hovorka, The application of ultrasonic waves to the study of electrolytic solutions. I. A

modification of debye's equation for the determination of the masses of electrolytic ions by means of ultrasonic waves, The Journal of Chemical Physics 15 (1947) 592. doi:10.1063/1.1746602.

[16] E. Yeager, J. Bugosh, F. Hovorka, J. McCarthy, The application of ultrasonic waves to the study of electrolytic solutions ii. the detection of the debye effect, The Journal of Chemical Physics 17 (1949) 411. doi:10.1063/1.1747269.

[17] R. Zana, E. Yeager, Ultrasonic vibration potentials and their use in the determination of ionic partial molal volumes, The Journal of Physical Chemistry 71 (1967) 521. doi:10.1021/j100862a010.

[18] S. Wang, C. K. Nguyen, G. J. Diebold, Ultrasonic vibration potential imaging: theory and experiments, in: A. A. Oraevsky, L. V. Wang (Eds.), Photons Plus Ultrasound: Imaging and Sensing 2007: The Eighth Conference on Biomedical Thermoacoustics, Optoacoustics, and Acousto-optics, volume 6437, International Society for Optics and Photonics, SPIE, 2007, pp. 169–173. doi:10.1117/12.694104.

[19] A. V. Kramarenko, G. P. Kulemin, A. M. Savchuk, Gemodinamicheskij komponent jelektrokardiogrammy, Biofizika 41 (1996) 686–694. URL: http://www.tredex-company.com/sites/default/files/images/1996.pdf.

[20] D. T. Blackstock, A. A. Atchley, Fundamentals of Physical Acoustics, Acoustical Society of America Journal 109 (2001) 1274–1276. doi:10.1121/1.1354982.

[21] H. J. Liebe, G. A. Hufford, T. Manabe, A model for the complex permittivity of water at frequencies below 1 THz, International Journal of Infrared and Millimeter Waves 12 (1991) 659–675. doi:10.1007/BF01008897.

[22] A. Stogryn, Equations for calculating the dielectric constant of saline water (correspondence), IEEE Transactions on Microwave Theory and Techniques 19 (1971) 733–736. doi:10.1109/TMTT.1971.1127617.

[23] S. Kleis, L. Sanchez, Dependence of speed of sound on salinity and temperature in concentrated nacl solutions, Solar Energy 45 (1990) 201–206. doi:10.1016/0038-092X(90)90087-S.

[24] D. J. Evans, D. J. Searles, S. R. Williams, Dissipation and the relaxation to equilibrium, Journal of Statistical Mechanics: Theory and Experiment 2009 (2009) P07029. doi:10.1088/1742-5468/2009/07/p07029.

[25] C. Alexander, M. Sadiku, Capacitors and inductors, in: Fundamentals of electric circuits, McGraw-hill Education, 2013, p. 992.

[26] A. Bacciotti, Stability and Control of Linear Systems, Studies in Systems, Decision and Control, Springer International Publishing, 2018. doi:10.1007/978-3-030-02405-5.

[27] M. Brin, G. Stuck, Introduction to Dynamical Systems, Cambridge University Press, 2002. doi:10.1017/CBO9780511755316.

[28] B. Y. Balagurov, Conduction of the three-dimensional model of a composite with structural anisotropy, Journal of Experimental and Theoretical Physics 123 (2016) 348–356. doi:10.1134/S1063776116060017.

[29] B. T. Kolomiets, V. M. Lyubin, V. P. Shilo, Anizotropy of the Electric Conductivity in Oriented Samples of Vitreous Semiconductors, Soviet Journal of Experimental and Theoretical Physics Letters 17 (1973) 412.

[30] G. Astarita, Thermodynamics and relaxation. the relationship between memory for past history and equilibrium, Journal of Membrane Science 3 (1978) 163–178. doi:10.1016/S0376-7388(00)83020-3.

[31] B. D. Coleman, V. J. Mizel, On thermodynamic conditions for the stability of evolving systems, Archive for Rational Mechanics and Analysis 29 (1968) 105–113. doi:10.1007/BF00281360.

[32] N. V. Ivanovskiy, L. N. Kozachenko, A. A. Ivanov, Tekhnicheskie sredstva sudovozhdeniya, FHBUOVO "KHMTU", 2020. arXiv:https://lib.kgmtu.ru/wp-content/uploads/no-category/5031.pdf.

[33] R. M. Umarkhodzhaev, Y. V. Pavlov, A. N. Vasil'ev, Istoriya razrabotki hiroskopa na osnove yadernoho mahnitnoho rezonansa v rossii v 1960–2000-e hody, Hiroskopiya i navihatsiya 26 (2018) 3–27. doi:10.17285/0869-7035.2018.26.1.003-027.

[34] J. Lighthill, Waves in fluids, Cambridge mathematical library, Cambridge University Press, 2001.

[35] A. V. Kramarenko, accessed: Nov 3, 2020", Demo of an industrial application (pump work control) of a non-contact rf registration device, URL: https://youtu.be/z-1pzf3iUyM.